Published in final edited form as:
Bone. 2009 April ; 44(4): 648–655. doi:10.1016/j.bone.2008.12.012.

Type 2 Diabetic Mice Demonstrate Slender Long Bones with Increased Fragility Secondary to Increased Osteoclastogenesis

Yuki Kawashima[*], **J. Christopher Fritton**[*], **Shoshana Yakar**, **Sol Epstein**, **Mitchell B. Schaffler**, **Karl J. Jepsen**, and **Derek LeRoith**

E-mail: Yuki Kawashima [yuki.kawashima@mssm.edu] J. Christopher Fritton [james.fritton@mssm.edu] Shoshana Yakar [shoshana.yakar@mssm.edu] Sol Epstein [bonedocsol@aol.com] Mitchell B. Schaffler [mitchell.schaffler@mssm.edu] Karl J. Jepsen [karl.jepsen@mssm.edu] Derek LeRoith

Abstract

Type 2 diabetics often demonstrate normal or increased bone mineral density, yet are at increased risk for bone fracture. Furthermore, the anti-diabetic oral thiazolidinediones (PPARγ agonists) have recently been shown to increase bone fractures. To investigate the etiology of possible structural and/or material quality defects, we have utilized a well-described mouse model of Type 2 diabetes (MKR). MKR mice exhibit muscle hypoplasia from birth with reduced mass by the pre-diabetic age of 3 weeks. A compensatory hyperplasia ensues during early (5 weeks) development; by 6–8 weeks muscle is normal in structure and function. Adult whole-bone mechanical properties were determined by 4-point bending to test susceptibility to fracture. Micro-computed tomography and cortical bone histomorphometry were utilized to assess static and dynamic indices of structure, bone formation and resorption.

Osteoclastogenesis assays were performed from bone marrow-derived non-adherent cells. The 8-week and 16-week, but not 3-week, male MKR had slender (i.e., narrow relative to length) femurs that were 20% weaker ($p<0.05$) relative to WT control femurs. Tissue-level mineral density was not affected. Impaired periosteal expansion during early diabetes resulted from 250% more, and 40% less of the cortical bone surface undergoing resorption and formation, respectively ($p<0.05$). Greater resorption persisted in adult MKR on both periosteal and endosteal surfaces. Differences were not limited to cortical bone as the distal femur metaphysis of 16 week MKR contained less trabecular bone and trabecular separation was greater than in WT by 60% ($p<0.05$). At all ages, MKR marrow-derived cultures demonstrated the ability for enhanced osteoclast differentiation in response to M-CSF and RANK-L. Taken together, the MKR mouse model suggests that skeletal fragility in Type 2 diabetes may arise from reduced transverse bone accrual and increased osteoclastogenesis during growth that is accelerated by the diabetic/hyperinsulinemic milieu. Further, these results emphasize the importance of evaluating diabetic bone based on morphology in addition to bone mass.

Keywords

bone fragility; bone histomorphometry; osteoclastogenesis; type 2 diabetes; mouse model

Corresponding author: Derek LeRoith, Division of Endocrinology, Diabetes and Bone Diseases, Mount Sinai School of Medicine, One Gustave L. Levy Place, New York, NY 10029, USA, Email : Derek.leroith@mssm.edu.
[*]Both of these authors contributed equally.

Conflict of Interest Statement: *The authors have nothing to disclose.*

Introduction

Diabetes is an emerging epidemic that has consequences for musculo-skeletal growth and development, and bone fracture risk [1–8]. Yet, Type 2 diabetics (non-insulin-dependent, T2D) often demonstrate increased bone mineral density (BMD) [9–13]. Furthermore, the use of anti-diabetic oral thiazolidinediones (PPARγ agonists) in T2D has recently been shown to increase fracture risk in the absence of a reduction in BMD [14]. These apparent paradoxes suggest that the increased bone fragility in T2D may not be discerned from bone mass, but may depend on aspects of bone structure or tissue quality that are not revealed from BMD. A number of factors have been postulated to be etiologically associated with poor bone accrual in diabetes, including an insulin-related direct reduction in bone formation and reduced force generating capacity of muscle.

Studies of bone turnover in animal models are most accurately assessed by histomorphometry. Several models have demonstrated diabetes-induced alterations in bone and could aid in elucidating the cellular and biomechanical mechanisms that may lead to increased risk of fragility fractures [15–20]. Models for Type 1 diabetes (T1D) are most prevalent and have demonstrated decreased breaking strength of femoral shafts when compared to controls [21, 22]. However, many of these are drug-induced models confounded by side-effects that can result in significant health issues. For example, the pancreatic β-cell toxins streptozotocin or alloxan have been injected into both rats and mice to induce an uncontrolled diabetic state [23,24]. Growth trajectories are immediately altered such that diabetic animals fail to grow (i.e., the rates of long bone growth and body mass gains are significantly stunted) [25,26]. However, stunted longitudinal growth is not normally associated with diabetes. Most recently, using a model of streptozotocin-induced insulinopenia, Hamada and co-workers confirmed this affect on growth as well as a reduction in trabecular bone volume with reduction in both bone formation and bone resorption in young animals, changes that were reversed by insulin replacement therapy [25]. The main conclusion of that study was that in T1D, insulinopenia is the primary etiology for osteopenia, though secondary mechanisms, such as oxidative stress, may also play a role [25]. The cellular mechanisms behind these differences require further examination.

Models of T2D have thus far been less biologically insightful because many induce obesity (another state of insulin resistance) or are limited to rats [27–30]. There is limited evidence for increased fracture risk due to greater levels of obesity and obesity may even protect a subject from fracture, despite being associated with lower physical activity [3]. Obesity increases the load-bearing forces during locomotion and, absent a bone formation defect, elicits structural compensation, i.e., more weight requires a larger frame [31]. Obesity may also enhance endogenous production of estrogen, a hormone important for bone cell regulation in both sexes [32]. Non-obese T2D occurs spontaneously in rats such as the Torii, which was outbred from Sprague-Dawley in 1997, and also exhibits stunted longitudinal bone growth; however, the disease has unknown etiology and is associated with insulinopenia [28].

We have generated a non-obese transgenic mouse model of T2D (MKR mice) by blocking both the insulin and IGF-signaling pathways specifically in skeletal muscle. Blocking of both receptors in muscle abrogates downstream signaling, particularly the AKT pathway, which regulates glucose uptake into muscle. MKR mice are born with *naturally* occurring hyperinsulinemia and insulin resistance in muscle. Early in life (~2 weeks) the MKR mice develop dyslipidemia, and the mice eventually develop frank diabetes with hyperglycemia (~7–8 weeks) [33,34]. This scenario of disease development is similar to the human disease, where insulin resistance and hyperinsulinemia, with dyslipidemia eventually progress to diabetes. The MKR mouse model is useful since no exogenous agents are required to induce disease,

thus removing potential confounding aspects. In addition, MKR mice are non-obese, excluding another confounding variable. In this study we employed the MKR mouse model to examine the effect of progression of T2D on skeletal integrity. Skeletal characterization was performed at the pre-diabetic (3 weeks of age), early diabetic (8 weeks) and established diabetic stages (16 weeks). Here we demonstrate that early onset of insulin resistance does not affect longitudinal growth but alters transverse expansion of skeletal structures, which worsens with the progression to the adult diabetic state.

Materials and Methods

The generation of the MKR Type 2 diabetic mouse has been described elsewhere [33]. MKR male mice, on a FVB/N background, were bred to homozygosity, and were compared to wild-type FVB/N controls (WT). MKR mice demonstrate severe insulin resistance starting at birth, hyperinsulinemia and hyperlipidemia at 3–4 weeks of age but with normoglycemia [33]. At 6–8 weeks of age MKR mice develop diabetes with blood glucose levels of 250–400 mg/dl versus 130–160 mg/dl for WT. The mice were kept on a 12-h light/dark cycle and were fed with standard chow ad libitum. All studies were conducted in accordance with NIH guidelines and approved by the Institutional Animal Care and Use Committee of the Mount Sinai School of Medicine.

Bone Histomorphometry

Cortical bone histomorphometry was carried out as described in detail elsewhere [35,36]. Briefly, control and MKR male mice at 3, 8 and 16 weeks of age were injected intraperitoneally with 10 mg/kg calcein (C-0875; Sigma) at 8 and 2 days prior to euthanasia to label bone forming surfaces. Left femurs were removed and fixed in 10% neutral buffered formalin, bulk-stained with Villanueva bone stain and embedded in poly-methylmethacrylate [35]. Embedded bones were sectioned transversely at the mid-diaphysis with a diamond-coated wafering saw, polished to a thickness of 30 μm with silicon carbide abrasive paper and mounted on glass slides. Cortical bone indices of osteoblast and osteoclast activity were measured using fluorescence and brightfield microscopy [35,37]. On both periosteal and endosteal surfaces, bone resorption was assessed from eroded surface (Er.Pm/B.Pm, %); bone formation was assessed by labeled surface (L.Pm/B.Pm, %), mineral apposition rate (MAR, μm/day), and bone formation rate (BFR/B.Pm, μm/day × 100). Sections were analyzed using an OsteoMeasure system (Osteometrics, Atlanta, GA, USA) connected to a Zeiss Axioskop microscope. A single observer blinded to the specimen identity made all measurements.

Micro-CT analysis

Three-dimensional micro-computed tomography (micro-CT) images of the contralateral (right) femurs for 3, 8 and 16 week old WT and MKR mice were obtained using an eXplore Locus SP Micro-CT system (GE Healthcare, London, Ontario, CA). Scans were performed at 15 μm isotropic voxel resolution as described elsewhere [38–40]. All scans were performed using a density calibration phantom containing air, water, and a hydroxyapatite standard (SB3; Gammex RMI, Middleton, WI, USA) to allow subsequent determinations of tissue mineral densities [39].

Mid-diaphyseal traits were quantified for a 2.5 mm diaphyseal region that was located immediately distal to the third trochanter. This site corresponded to the typical location of failure during the bending tests (see below). The mid-diaphyseal morphological traits measured were the tissue amounts (cortical area, Ct.Ar; marrow area, Ma.Ar; total area, Tt.Ar; cortical width, Ct.Wi), perimeters (endosteal, Es.Pm; periosteal, Ps.Pm) and the spatial distribution of mineralized tissue (polar moment of inertia, J). Moment of inertia is a measure of the proximity of the tissue to the geometric centroid of the cross-section. Total area was defined as the sum

of the cortical and marrow areas. Traits were quantified for each cross-section and the values were averaged. Hind-limb long bone lengths were measured as the caliper distance between the proximal and distal most articulating surfaces (0.01 mm resolution). Micro-CT was also used to quantify tissue mineralization as described above [39]. Tissue mineral density (TMDn, mg/cc) was determined by converting grayscale values to mineral density values using a density calibration curve from the scanned phantom and then averaging mineral content values over all thresholded “bone” voxels.

Trabecular architecture was quantified for the proximal and distal femoral metaphyses. Cortical and trabecular bone were segmented manually and the trabecular volumes were filtered using a median-filtering algorithm and then thresholded. Trabecular traits measured include trabecular bone volume fraction (BV/TV), thickness (Tb.Th), and separation (Tb.Sp).

Whole bone mechanical properties

To understand the effects of dysregulated carbohydrate and lipid metabolism on adult skeletal strength, mechanical properties were quantified by loading 16 week-old mouse femurs to failure. Following the micro-CT scans, right femurs were loaded in 4-point bending at 0.05 mm/sec using a servo-hydraulic materials test system (Instron Corporation, Norwood, MA, USA) to assess whole bone mechanical properties [41]. Femurs were tested at room temperature and kept moist with phosphate-buffered saline. Load-deflection curves were analyzed for stiffness (the slope of the initial linear portion of the curve), maximum load (Failure Load), and post-yield deflection (PYD). Yield was defined as a 10% reduction of secant stiffness (load range normalized for deflection range) relative to the initial (tangent) stiffness. PYD, a measure of ductility, was defined as the deflection at failure minus the deflection at yield.

Marrow-derived osteoclast cultures

Bone marrow stromal cells were isolated from whole bone marrow immediately after euthanasia of 4, 8 and 16 week-old mice. Cells were flushed out with a syringe and 26-gauge needle and collected in primary culture medium (aMEM). The marrow cell suspension was drawn through an 18-gauge needle to achieve single cell suspension. Cells were then washed in primary culture medium and cultured overnight in αMEM supplemented with 10% heat-inactivated fetal bovine serum [42]. Non-adherent cells were collected, washed and plated at a constant density (3×10^4 cells/well) in 96-well plastic plates with M-CSF (30 ng/ml) and RANKL (60 ng/ml) to allow for cell proliferation and differentiation, respectively. Tartrate resistant acid phosphatase (TRAP) staining was carried out using a Sigma kit, (Sigma 387-A) according to the manufacturer’s instructions. TRAP positive, multi-nucleated (>3 nuclei per cell) osteoclasts were counted.

RNA extraction and reverse transcription (RT) –PCR

Total RNA was isolated from osteoclast cultures using a QIAGEN RNA Midi kit (QIAGEN Inc., Valencia, CA, USA) and quantified by spectrophotometry. RNA integrity was verified using Bioanalyzer (Agilent Technologies 2100 Bioanalyzer-Bio Sizing, Version A.02.12 SI292). Quantitative real-time PCR: One μg of RNA obtained marrow-derived osteoclast cultures was transcribed to cDNA using oligo(dT) primers with RT-PCR kit according to the manufacturer’s instructions (Invitrogen Corp., Carlsbad, CA, USA). Real-time PCR was performed with the QuantiTect™ SYBR® green PCR kit (Qiagen, Valencia, CA, USA) according to the manufacturer’s instructions in ABI PRISM 7900HT sequence detection systems (Applied Biosystems, Foster City, CA USA). Primers: TRAP (5′-CACGAGAGTCCTGCTTGTC-3′ and 5′-AGTTGGGCATACTTC-3′), Cathepsin K (5′-CAGCAGAGGTGTGTACTATG-3′ and 5′-GCGTTGTTCTTATTCCGAGC-3′), β-actin (5′-TGTTACCAACTGGGACGACA-3′ and 5′-GGGGTGTTGAAGGTCTCAAA-3′)

Statistics

Differences in morphological, mechanical, and cell-behavior related trait values among the MKR and WT, three time points and anatomical locations were assessed individually by two-way analysis of variance (ANOVA) with interaction. The type I error rate (α) was set at 0.05. Significant interaction terms justified comparing differences between MKR and WT at individual time points using post-hoc Bonferroni-adjusted multiple comparisons (SYSTAT Software, SPSS Science, Chicago, IL USA). Analysis of the histomorphometric data was conducted using StatView (Cary, NC, USA).

Results

Diabetes phenotype of MKR mice

Male MKR and FVB/N control mice (WT) were weaned at 3 weeks of age and following genotyping as previously described were monitored weekly for blood glucose levels [33]. All mice remained normoglycemic from 3 weeks to 5 weeks of age. By 7 weeks of age, fed blood glucose levels in MKR mice rose to diabetic levels (between 250–400 mg/dl), whereas WT remained normoglycemia (between 130–160 mg/dl). The hyperglycemia of the MKR mice remained at 16 weeks of age. Hyperlipidemia and hyperinsulinemia levels in the MKR mice were seen at the pre-diabetic ages and remained throughout the study, as previously reported [33].

Early onset of type 2 diabetes leads to reduced strength and stiffness at adulthood

MKR mice had weaker and less stiff femurs compared to WT. Maximum load sustained at fracture by the MKR femurs was 20% lower than WT (Figure 1A). Similarly, stiffness was 24% lower for MKR femurs. MKR femurs exhibited greater ductility as measured by an approximately 50% increase in post-yield deflection (PYD), suggesting tissue properties were altered in MKR mice. PYD reflects the amount of deflection that occurs after structural damage is initiated but before complete failure by fracture. Together, these data show that diabetic MKR femora were weaker and less stiff compared to WT femora

Reduced stiffness of the MKR bones is due to increased slenderness

MKR femurs showed growth-related suppression of periosteal expansion, which coincided with the progression to diabetes between 6 to 8 weeks. MKR femur and tibia lengths were not significantly different than WT (Figure 1B) indicating that longitudinal growth was not affected at all three time-points critical to the progression of diabetes. However, MKR femurs at 8 and 16 weeks had smaller cross-sectional traits, indicating that MKR cortical bone was more slender compared to WT. The slender bone phenotype arose during a period of periosteal expansion normally associated with longitudinal growth and transverse expansion in mice between 3 and 8 weeks of age. At 3 weeks of age, MKR and WT femurs were not significantly different in any cortical trait measured by micro-CT (Table 1). Both the 8- and 16-week MKR femurs had smaller total, marrow and cortical areas (Tt.Ar, Ma.Ar and Ct.Ar). Tt.Ar has a large influence on all other cross-sectional properties and reflects the overall width of the mid-shaft. Tt.Ar is largely influenced by the temporal sequence of osteoblastic and osteoclastic activity that expands the periosteal surface during growth and further moves the surface (cortical drift) throughout adulthood. In addition to Ma.Ar and Ct.Ar the other cross-sectional properties influenced by Tt.Ar include cortical width (Ct.Wi), endosteal and periosteal perimeters (Es.Pm and Ps.Pm), and polar moment of inertia (J) (Figure 1C and D). Further, the micro-CT analysis revealed that the reduced failure load and stiffness seen in the mechanical testing of adult mouse femurs were associated with a 19% lower polar moment of inertia (Figure 1D). No differences in bone tissue-level mineral density (TMDn) were found in the MKR bones at any age (Table

1), indicating that the degree of mineralization was not affected during the progression to diabetes.

Increased osteoclast activity in bones of MKR mice contributes to the slender adult phenotype

Periosteal surface—Consistent with equivalent total areas at 3 weeks of age, osteoclast and osteoblast activity at the periosteal surface (% of eroded and labeled perimeter, Er.Pm and L.Pm, respectively) were not significantly different between MKR and WT mice (Figure 2). However, the lower Tt.Ar of MKR femurs that arose during growth after 3 weeks of age was associated with markedly increased periosteal resorption (Er.Pm increased ~3 fold by 8 weeks of age in MKR) compared to WT mice and significantly decreased perisosteal formation, (L.Pm and MAR were reduced 25% and 21%, respectively, $p<0.05$) resulting in a 39% lower bone formation rate. By 16 weeks of age, periosteal osteoblastic differences (L.Pm and MAR) were absent, but resorption (Er.Pm) in MKR was remained nearly 200% greater than in WT. The increase in osteoclastic activity is consistent with the maintenance of the slender-MKR phenotype between 8 and 16 weeks of age.

Endocortical Surface—Osteoclastic activity patterns at the endocortical surface were increased in MKR femurs similar to the periosteal surface; Er.Pm on the endosteal surface was elevated (80%) in MKR compared to WT at 3 weeks and remained elevated for MKR (>100% WT) throughout growth and development in similar fashion to Er.Pm on the periosteal surface (Figure 2). Osteoblastic measures (L.Pm and MAR) were not different between MKR and WT mice at any age on the endosteal surface (Figure 2).

MKR mice lose cancellous bone with the progression of diabetes

Micro-CT studies revealed the largest effect on bone volume fraction to be in the distal femoral metaphyses where cancellous BV/TV was 40% lower in MKR compared to WT at 16 weeks of age (Table 2). This lower BV/TV reflected an altered microarchitecture in the MKR distal femur with significantly greater trabecular separation (60%) compared to WT, consistent with increased osteoclastic activity and loss of trabeculae. At 3 weeks of age the proximal metaphysis, but not the distal metaphysis, of MKR femurs contained less cancellous bone compared to WT (Table 2). The reduced bone volume fraction persisted into adulthood. By 16 weeks, significant differences were apparent in trabecular thickness (−36%) and separation (58%) between the MKR and WT proximal metaphysis.

Increased number of osteoclast precursors in marrow of MKR mice

To unravel the cellular mechanism involved in decreased cortical and cancellous bone in MKR mice, we studied bone marrow-derived osteoclast cultures. Osteoclast cultures (Figure 3) derived from MKR mice exhibited an increase in osteoclast numbers at 4, 8 and 16 weeks, as determined by TRAP staining. Expression of the osteoclast markers including TRAP and Cathepsin K were increased in cultures derived from MKR mice at 8 and 16 weeks of age.

Discussion

Fragility fractures are associated with both Type 1 and 2 diabetes despite the fact that bone mass (BMD) losses *do not* occur in Type 2 diabetes (T2D) [9–13]. The reductions in BMD with Type 1 diabetes (T1D) occur early in the disease process and are associated with increased bone fragility and fractures later in life. While the reductions in BMD in T1D have been well established, the cellular cause(s) have not been defined completely, with both increased bone turnover and decreased osteoblastic activity implicated in the net bone loss [43]. In contrast, there is no conspicuous reduction in BMD in T2D [10]. Thus, the increase in fragility fractures in T2D is more likely the result of changes in bone integrity and/or quality. Indeed, our

biomechanical studies in the hyperglycemic MKR mice support this concept, with significantly altered relative fracture toughness (as measured from post-yield deflection) and reduced overall bone stiffness and strength in the diseased state. Mechanical data from other T2D models are unavailable for comparison. The observed changes in stiffness and strength in these studies are largely accounted for by the changes in morphology and consistent with the smaller cross-sectional sizes (Tt.Ar and J) of MKR bone compared to WT. That MKR femurs are more slender (narrow relative to length) is an important finding because slenderness in human bone has been shown to be a significant indicator of fracture risk [44–48].

We have now identified both muscle and bone deficiencies in the MKR mouse albeit first presenting at different ages. The MKR mouse exhibits muscle hypoplasia with a 20% lower protein content in soleus and extensor digitorum longus early in life at 3 weeks of age. Interestingly, by 5–6 weeks, compensatory mechanisms are at work as shown recently by skeletal muscle hypertrophy and strengthening [34,49]. Therefore, even before frank diabetes appears at ~7–8 weeks, skeletal muscle approximates that of WT but with protein content that is 15% higher in MKR than in WT mice at 5 weeks of age [34,49]. Thus, it is conceivable that the bone structural effects seen at 8 and 16 weeks of age arose early in growth when the effects of hypoplastic skeletal muscle may affect bone structure. However, despite the muscle deficit there was no significant difference in femoral cortical bone characteristics between MKR and WT mice at 3 weeks of age. Moreover, as insulin resistance in the MKR mice progressed and skeletal muscle function improved at 8 and 16 weeks, MKR mice demonstrated significant structural impairments in skeletal integrity compared to WT mice, reflected by reduced cortical bone size and trabecular bone volume. This strongly argues that the progression of the MKR mice to the Type 2 diabetic state played a role in these bone structural changes.

Hyperglycemia and hyperinsulinemia have been postulated as possible causes of skeletal changes in diabetic patients. While the mechanism(s) are not known, advanced glycosylation end products (AGEs) working through their specific receptors (RAGE) [19] have been postulated to alter bone cell function. Hyperglycemia suppresses osteoblast proliferation and differentiation in culture systems, and the mechanisms may involve expression of c-jun, a transcription factor that affects collagen expression in bone-derived cell lines [50,51]. Insulin is aparently a hormone important for osteoblast function, chondrogenesis and collagen synthesis, and may also be involved in osteoclastogenesis [52]. Fracture risk has been shown to increase with insulin use [7,8,53,54]. However, in mouse models of insulinopenia (T1D), reduced serum osteocalcin and lower bone osteoblast numbers are associated with reduced osteoid and reduced bone mineral accretion rates, resulting in lower bone turnover rates. In a model of T2D, a knockout mouse for the insulin receptor (IR), BMD was normal, possibly compensated for by the IGF-1R or perhaps demonstrating a lesser role of the insulin resistance in bone formation [55].

Other features of the T2D milieu beyond AGEs are yet to be fully studied regarding their impact on bone, such as lipids and oxidative stress. In two separate models, one a streptozotocin diabetic mouse and one a rat model of non-obese, insulin-sensitive T2D, osteopenia was demonstrated. In both models oxidative stress markers were measured and found to be elevated and normalized with insulin therapy. In the former model, the oxidative stress marker (8-OHdG) was also seen to be increased in bone by immunohistochemical analysis, and the authors speculated that the inhibition of osteoblastic differentiation could be explained by this effect [25,28]. Indeed, oxidative stress may affect osteoblastic differentiation as demonstrated in vitro [56,57]. In our laboratory, MKR mice also demonstrate increased oxidative stress markers in serum and liver (unpublished), and this potential pathogenic factor and its effect on bone formation and bone turnover requires more extensive study.

The principal bone cell defect in MKR mice is increased osteoclastogenesis, particularly at later ages, as demonstrated in the current study both by histomorphometry as well as bone marrow cultures. The slender bones in the MKR diaphyses, as well as the reduced cancellous bone volume and increased trabecular separation appear to result principally from increased osteoclastic activity and a small transient suppression of osteoblastic activity. That marked increases in cell differentiation were present in vitro, in the absence of the circulating endocrine milieu of T2D, suggests that the factors associated with the diabetes in the MKR mice (e.g., insulin resistance, hyperglycemia) may cause a shift in the marrow osteoclast precursor pool or a phenotypic shift in the sensitivity of the precursors to osteoclast regulatory factors.

Despite a paucity of data, there has been general acceptance of the view that increased activity by osteoclasts does not play a role in T2D-related bone disease because of low bone turnover. Based on clinical biopsy bone formation data from a heterogeneous population (body mass index, sex and ancestry) Krakauer *et al.* speculated that the metabolic effects of poor glycemic control leads to increased bone resorption, but then low bone turnover retards age-related bone loss [58]. While such site-specific data is missing from the more recent clinical literature, biochemical data support the view that osteoclastic function is accelerated in non-obese males with T2D [59]. Resolution of this issue in human subjects remains for future studies. Current data from the MKR mice, as well as prior studies of T2D rats [27,30] also argue that alteration in osteoclast action may be present, though their contribution to the bone fragility in this disease remain unclear.

The biomechanical results from the current studies show that MKR bones were significantly weaker and less stiff than WT femurs. These changes are attributable to the smaller bone size and cross-sectional moment of inertia of the MKR bones. However, we also observed changes in the fracture resistance (ductility) of the MKR bones that suggest there is also a significant alteration in tissue quality of the diabetic bone. Specifically, the MKR femurs exhibited approximately 50% greater post-yield deflection (PYD) than WT. Compositionally, such changes can result from decreased mineral content, but this was not seen in the mineralization measurements of MKR bones. Alternatively, increases in bone collagen content or alterations in collagen cross-linking with other matrix constituents can also produce these changes in fracture behavior; however these could not be examined directly in the current studies because of the limits imposed by the other investigational techniques used.

Although osteoporotic fracture is more prevalent in women, the effects on men often result in greater morbidity and mortality, principally because related fractures occur later in life and males have a greater co-morbidity risk [60]. In several clinical studies fracture risk associated with diabetes appears to differ between men and women; diabetes was associated independently with increasing risk of non-vertebral fractures among men but not women [9, 61,62]. Male diabetics are also more prone to be non-obese and the sexual dimorphism may be related to obesity and greater androgenecity in women with hyperglycemic and hyperinsulinemic conditions [9,62]. Nonetheless, the increased male risk cannot be explained as an effect of BMD; both men and women with T2D had similar BMD compared to normals. In men, there is an increased risk associated with T2D of short duration that has not yet been attributed to reduced bone mass, quality or some other factor [2]. For these reasons we choose to study male animals, as have many previous researchers, and all studies should be repeated in females [26].

While our MKR mice are smaller than WT, both groups exhibited normal and similar weight gain from 3 to 16 weeks of age (MKR: 177%, WT: 173%). This is in contrast to the drug-induced diabetic animals that exhibit metabolic abnormalities characteristic of uncontrolled diabetes, including body weight gain [26]. Previous work has established that tissue wet weights of organs expressing IGF-I receptors, namely, brain, lung, heart, liver, spleen, kidney,

perigonadal white fat, and skeletal muscle are not different between MKR and WT mice, except for total skeletal muscle from birth to 5 weeks, and muscle mass differences between MKR and WT mice resolve; similar muscle weight and strength are seen when measured at 8 weeks [34]. Thus, the MKR mice allow the separation of the hyperglycemic and hyperinsulinemic effects from increases in body weight and adiposity.

In summary, we presented a mouse model of T2D, which progresses from severe insulin resistance to frank diabetes. The early onset of the disease, during adolescence and puberty, lead to slender adult bones resulting in reduced strength and stiffness, and also changes in fracture resistance. The slender bones in diabetic mice resulted principally from increases in osteoclastic activity, increases that paralleled the progression to diabetes. Cortical and cancellous bone responded similarly, with loss of bone mass and trabecular architecture in concert with the progression to diabetes. These data suggest that T2D results in a complex array of alterations to skeletal morphology (resulting from net resorptive cellular activity) and tissue composition that may not be readily assessed (i.e., DEXA) or treated (i.e., anti-resorptive or bone anabolic strategies) using traditional measures. Whether control of the hyperglycemia and/or insulin resistance will resolve these skeletal issues awaits further research.

Acknowledgements

We are indebted to Ken Inagaki, Damien Laudier, Valerie Williams, David Berman, and Bin Hu for their help on this project. Financial support received from funding agencies in the United States including the Mount Sinai School of Medicine (Steckler Fund Grant to DL), NIAMS (NIH Grants AR41210 to MBS, AR44927 to KJJ and AR054919 & AR055141 to SY), National Space Biomedical Research Institute (NASA Grant NCC 9–58 to MBS) and the Charles H. Revson Foundation (Fellowship to JCF). The statements made and views expressed, however, are solely the responsibility of the authors.

Abbreviations

8-OHdG
: 8-hydroxydeoxyguanosine, an oxidized nucleoside of DNA

αMEM
: α-modified Minimum Essential Medium

AGE
: Advanced Glycation End products

BMD
: areal Bone Mineral Density measured by DEXA

DEXA
: Dual Energy X-ray Absorptiometry

FVB/N
: Friend Virus B NIH inbreed strain of mouse, WT

IGF
: Insulin-like Growth Factor

IR
: Insulin Receptor

J
: cross-sectional polar moment of inertia

M-CSF

Macrophage-Colony-Stimulating Factor

Micro-CT
Micro-Computed Tomography

MKR
Muscle creatine Kinase promoter/human IGF-I Receptor

MSC
Marrow Stromal Cell

PPARγ
Peroxisome Proliferator-Activated Receptor γ

PYD
Post-Yield Deflection

RAGE
Receptors specific for AGE proteins

RANKL
Receptor Activator of Nuclear factor-κβLigand

T1D
Type 1 Diabetes Mellitus

T2D
Type 2 Diabetes Mellitus

TRAP
Tartrate Resistant Acid Phosphatase

WT
Wild-Type, FVB/N

Histomorphometry Abbreviations[37]

B.Pm
Bone Perimeter

BV/TV
Bone Volume Fraction for cancellous bone

Ct.Ar
cross-sectional Cortical Area

Ct.Wi
cross-sectional Cortical Width

Er.Pm
cross-sectional Eroded Perimeter

Es.Pm
cross-sectional Endosteal Perimeter

dL.Pm
cross-sectional double Labeled Perimeter

sL.Pm

cross-sectional single Labeled Perimeter

L.Pm
cross-sectional Labeled Perimeter = dL.Pm+sL.Pm/2

MAR
Mineral Apposition Rate

BFR
Bone Formation Rate=MAR*L.Pm/B.Pm

Ps.Pm
cross-sectional Periosteal Perimeter

Tb.Sp
Trabecular Separation

Tb.Th
Trabecular Thickness

Tt.Ar
cross-sectional Total Area

Ma.Ar
cross-sectional Marrow Area

TMDn
Tissue Mineral Density measured by micro-CT

References

1. Boyle JP, Honeycutt AA, Narayan KM, Hoerger TJ, Geiss LS, Chen H, Thompson TJ. Projection of diabetes burden through 2050: impact of changing demography and disease prevalence in the U.S. Diabetes Care 2001;24:1936–40. [PubMed: 11679460]
2. Forsen L, Meyer HE, Midthjell K, Edna TH. Diabetes mellitus and the incidence of hip fracture: results from the Nord-Trondelag Health Survey. Diabetologia 1999;42:920–5. [PubMed: 10491750]
3. Gunczler P, Lanes R, Paz-Martinez V, Martins R, Esaa S, Colmenares V, Weisinger JR. Decreased lumbar spine bone mass and low bone turnover in children and adolescents with insulin dependent diabetes mellitus followed longitudinally. J Pediatr Endocrinol Metab 1998;11:413–19. [PubMed: 11517957]
4. Hofbauer LC, Brueck CC, Singh SK, Dobnig H. Osteoporosis in patients with diabetes mellitus. J Bone Miner Res 2007;22:1317–28. [PubMed: 17501667]
5. Inzerillo AM, Epstein S. Osteoporosis and diabetes mellitus. Rev Endocr Metab Disord 2004;5:261–8. [PubMed: 15211098]
6. Kemink SA, Hermus AR, Swinkels LM, Lutterman JA, Smals AG. Osteopenia in insulin-dependent diabetes mellitus; prevalence and aspects of pathophysiology. J Endocrinol Invest 2000;23:295–303. [PubMed: 10882147]
7. Melton LJ, Leibson CL, Achenbach SJ, Therneau TM, Khosla S. Fracture risk in type 2 diabetes: Update of a population-based study. J Bone Miner Res 2008;23:1334–42. [PubMed: 18348689]
8. Nicodemus KK, Folsom AR. Type 1 and type 2 diabetes and incident hip fractures in postmenopausal women. Diabetes Care 2001;24:1192–7. [PubMed: 11423501]
9. Buysschaert M, Cauwe F, Jamart J, Brichant C, De Coster P, Magnan A, Donckier J. Proximal femur density in type 1 and 2 diabetic patients. Diabete Metab 1992;18:32–7. [PubMed: 1563534]
10. de L II, van der Klift M, de Laet CE, van Daele PL, Hofman A, Pols HA. Bone mineral density and fracture risk in type-2 diabetes mellitus: the Rotterdam Study. Osteoporos Int 2005;16:1713–20. [PubMed: 15940395]

11. Lipscombe LL, Jamal SA, Booth GL, Hawker GA. The risk of hip fractures in older individuals with diabetes: a population-based study. Diabetes Care 2007;30:835–41. [PubMed: 17392544]
12. Schwartz AV, Sellmeyer DE, Strotmeyer ES, Tylavsky FA, Feingold KR, Resnick HE, Shorr RI, Nevitt MC, Black DM, Cauley JA, Cummings SR, Harris TB. Diabetes and bone loss at the hip in older black and white adults. J Bone Miner Res 2005;20:596–603. [PubMed: 15765178]
13. Vestergaard P, Rejnmark L, Mosekilde L. Increased mortality in patients with a hip fracture-effect of pre-morbid conditions and post-fracture complications. Osteoporos Int 2007;18:1583–44. [PubMed: 17566814]
14. Kahn SE, Haffner SM, Heise MA, Herman WH, Holman RR, Jones NP, Kravitz BG, Lachin JM, O'Neill MC, Zinman B, Viberti G, Group AS. Glycemic durability of rosiglitazone, metformin, or glyburide monotherapy. N Engl J Med 2006;355:2427–43. [PubMed: 17145742]
15. Almeida M, Han L, Martin-Millan M, Plotkin LI, Stewart SA, Roberson PK, Kousteni S, O'Brien CA, Bellido T, Parfitt AM, Weinstein RS, Jilka RL, Manolagas SC. Skeletal involution by age-associated oxidative stress and its acceleration by loss of sex steroids. J Biol Chem 2007;282:27285–97. [PubMed: 17623659]
16. Bouxsein ML, Rosen CJ, Turner CH, Ackert CL, Shultz KL, Donahue LR, Churchill G, Adamo ML, Powell DR, Turner RT, Muller R, Beamer WG. Generation of a new congenic mouse strain to test the relationships among serum insulin-like growth factor I, bone mineral density, and skeletal morphology in vivo. J Bone Miner Res 2002;17:570–9. [PubMed: 11918215]
17. Campos Pastor MM, Lopez-Ibarra PJ, Escobar-Jimenez F, Serrano Pardo MD, Garcia-Cervigon AG. Intensive insulin therapy and bone mineral density in type 1 diabetes mellitus: a prospective study. Osteoporos Int 2000;11:455–9. [PubMed: 10912849]
18. Jiang J, Lichtler AC, Gronowicz GA, Adams DJ, Clark SH, Rosen CJ, Kream BE. Transgenic mice with osteoblast-targeted insulin-like growth factor-I show increased bone remodeling. Bone 2006;39:494–504. [PubMed: 16644298]
19. Miyata T, Notoya K, Yoshida K, Horie K, Maeda K, Kurokawa K, Taketomi S. Advanced glycation end products enhance osteoclast-induced bone resorption in cultured mouse unfractionated bone cells and in rats implanted subcutaneously with devitalized bone particles. J Am Soc Nephrol 1997;8:260–70. [PubMed: 9048345]
20. Phornphutkul C, Wu K-Y, Gruppuso PA. The role of insulin in chondrogenesis. Mol Cell Endocrinol 2006;249:107–15. [PubMed: 16530934]
21. Einhorn TA, Boskey AL, Gundberg CM, Vigorita VJ, Devlin VJ, Beyer MM. The mineral and mechanical properties of bone in chronic experimental diabetes. J Orthop Res 1988;6:317–23. [PubMed: 3258636]
22. Hou JC, Zernicke RF, Barnard RJ. Experimental diabetes, insulin treatment, and femoral neck morphology and biomechanics in rats. Clin Orthop Relat Res 1991:278–85. [PubMed: 1997247]
23. Schneider LE, Schedl HP. Diabetes and intestinal calcium absorption in the rat. Am J Physiol 1972;223:1319–23. [PubMed: 4641621]
24. Schneider LE, Wilson HD, Schedl HP. Intestinal calcium binding protein in the diabetic rat. Nature 1973;245:327–8. [PubMed: 4586441]
25. Hamada Y, Kitazawa S, Kitazawa R, Fujii H, Kasuga M, Fukagawa M. Histomorphometric analysis of diabetic osteopenia in streptozotocin-induced diabetic mice: a possible role of oxidative stress. Bone 2007;40:1408–14. [PubMed: 17251074]
26. Reddy GK, Stehno-Bittel L, Hamade S, Enwemeka CS. The biomechanical integrity of bone in experimental diabetes. Diabetes Res Clin Pract 2001;54:1–8. [PubMed: 11532324]
27. Amir G, Rosenmann E, Sherman Y, Greenfeld Z, Ne'eman Z, Cohen AM. Osteoporosis in the Cohen diabetic rat: correlation between histomorphometric changes in bone and microangiopathy. Lab Invest 2002;82:1399–405. [PubMed: 12379774]
28. Fujii H, Hamada Y, Fukagawa M. Bone formation in spontaneously diabetic Torii-newly established model of non-obese type 2 diabetes rats. Bone 2008;42:372–9. [PubMed: 18037364]
29. Koh EH, Kim MS, Park JY, Kim HS, Youn JY, Park HS, Youn JH, Lee KU. Peroxisome proliferator-activated receptor (PPAR)-alpha activation prevents diabetes in OLETF rats: comparison with PPAR-gamma activation. Diabetes 2003;52:2331–7. [PubMed: 12941773]

30. Verhaeghe J, Visser WJ, Einhorn TA, Bouillon R. Osteoporosis and diabetes: lessons from the diabetic BB rat. Horm Res 1990;34:245–8. [PubMed: 2100283]

31. Beck TJ, Oreskovic TL, Stone KL, Ruff CB, Ensrud K, Nevitt MC, Genant HK, Cummings SR. Structural adaptation to changing skeletal load in the progression toward hip fragility: the study of osteoporotic fractures. J Bone Miner Res 2001;16:1108–19. [PubMed: 11393788]

32. Riggs BL, Khosla S, Melton LJ 3rd. Sex steroids and the construction and conservation of the adult skeleton. Endocr Rev 2002;23:279–302. [PubMed: 12050121]

33. Fernandez AM, Kim JK, Yakar S, Dupont J, Hernandez-Sanchez C, Castle AL, Filmore J, Shulman GI, Le Roith D. Functional inactivation of the IGF-I and insulin receptors in skeletal muscle causes type 2 diabetes. Genes Dev 2001;15:1926–34. [PubMed: 11485987]

34. Fernandez AM, Dupont J, Farrar RP, Lee S, Stannard B, Le Roith D. Muscle-specific inactivation of the IGF-I receptor induces compensatory hyperplasia in skeletal muscle. J Clin Invest 2002;109:347–55. [PubMed: 11827994]

35. Li CY, Schaffler MB, Wolde-Semait HT, Hernandez CJ, Jepsen KJ. Genetic background influences cortical bone response to ovariectomy. J Bone Miner Res 2005;20:2150–8. [PubMed: 16294268]

36. Li CY, Jepsen KJ, Majeska RJ, Zhang J, Ni R, Gelb BD, Schaffler MB. Mice lacking cathepsin K maintain bone remodeling but develop bone fragility despite high bone mass. J Bone Miner Res 2006;21:865–75. [PubMed: 16753017]

37. Parfitt AM, Drezner MK, Glorieux FH, Kanis JA, Malluche H, Meunier PJ, Ott SM, Recker RR. Bone histomorphometry: standardization of nomenclature, symbols, and units. Report of the ASBMR Histomorphometry Nomenclature Committee. J Bone Miner Res 1987;2:595–610. [PubMed: 3455637]

38. Fritton JC, Myers ER, Wright TM, van der Meulen MC. Loading induces site-specific increases in mineral content assessed by microcomputed tomography of the mouse tibia. Bone 2005;36:1030–8. [PubMed: 15878316]

39. Jepsen KJ, Hu B, Tommasini SM, Courtland H-W, Price C, Terranova CJ, Nadeau JH. Genetic randomization reveals functional relationships among morphologic and tissue-quality traits that contribute to bone strength and fragility. Mamm Genome 2007;18:492–507. [PubMed: 17557179]

40. Tommasini SM, Morgan TG, van der Meulen M, Jepsen KJ. Genetic variation in structure-function relationships for the inbred mouse lumbar vertebral body. J Bone Miner Res 2005;20:817–27. [PubMed: 15824855]

41. Jepsen KJ, Akkus OJ, Majeska RJ, Nadeau JH. Hierarchical relationship between bone traits and mechanical properties in inbred mice. Mamm Genome 2003;14:97–104. [PubMed: 12584605]

42. Toyoshima Y, Karas M, Yakar S, Dupont J, Lee H, LeRoith D. TDAG51 mediates the effects of insulin-like growth factor I (IGF-I) on cell survival. J Biol Chem 2004;279:25898–904. [PubMed: 15037619]

43. McCabe LR. Understanding the pathology and mechanisms of type I diabetic bone loss. J Cell Biochem 2007;102:1343–57. [PubMed: 17975793]

44. Beck TJ, Ruff CB, Shaffer RA, Betsinger K, Trone DW, Brodine SK. Stress fracture in military recruits: gender differences in muscle and bone susceptibility factors. Bone 2000;27:437–44. [PubMed: 10962357]

45. Crossley K, Bennell KL, Wrigley T, Oakes BW. Ground reaction forces, bone characteristics, and tibial stress fracture in male runners. Med Sci Sports Exerc 1999;31:1088–93. [PubMed: 10449008]

46. Duan Y, Seeman E, Turner CH. The biomechanical basis of vertebral body fragility in men and women. J Bone Miner Res 2001;16:2276–83. [PubMed: 11760842]

47. Giladi M, Milgrom C, Simkin A, Stein M, Kashtan H, Margulies J, Rand N, Chisin R, Steinberg R, Aharonson Z, et al. Stress fractures and tibial bone width. A risk factor. J Bone Joint Surg Br 1987;69:326–9. [PubMed: 3818769]

48. Gilsanz V, Loro ML, Roe TF, Sayre J, Gilsanz R, Schulz EE. Vertebral size in elderly women with osteoporosis. Mechanical implications and relationship to fractures. J Clin Invest 1995;95:2332–7. [PubMed: 7738196]

49. Spangenburg EE, Le Roith D, Ward CW, Bodine SC. A functional insulin-like growth factor receptor is not necessary for load-induced skeletal muscle hypertrophy. J Physiol 2008;586:283–91. [PubMed: 17974583]

50. Balint E, Szabo P, Marshall CF, Sprague SM. Glucose-induced inhibition of in vitro bone mineralization. Bone 2001;28:21–8. [PubMed: 11165939]
51. Zayzafoon M, Stell C, Irwin R, McCabe LR. Extracellular glucose influences osteoblast differentiation and c-Jun expression. J Cell Biochem 2000;79:301–10. [PubMed: 10967557]
52. Bouillon R, Bex M, Van Herck E, Laureys J, Dooms L, Lesaffre E, Ravussin E. Influence of age, sex, and insulin on osteoblast function: osteoblast dysfunction in diabetes mellitus. J Clin Endocrinol Metab 1995;80:1194–202. [PubMed: 7714089]
53. Ottenbacher KJ, Ostir GV, Peek MK, Goodwin JS, Markides KS. Diabetes mellitus as a risk factor for hip fracture in mexican american older adults. J Gerontol A Biol Sci Med Sci 2002;57:M648–53. [PubMed: 12242318]
54. Vestergaard P, Rejnmark L, Mosekilde L. Relative fracture risk in patients with diabetes mellitus, and the impact of insulin and oral antidiabetic medication on relative fracture risk. Diabetologia 2005;48:1292–9. [PubMed: 15909154]
55. Irwin R, Lin HV, Motyl KJ, McCabe LR. Normal bone density obtained in the absence of insulin receptor expression in bone. Endocrinology 2006;147:5760–7. [PubMed: 16973725]
56. Bai, X-c; Lu, D.; Bai, J.; Zheng, H.; Ke, Z-y; Li, X-m; Luo, S-q. Oxidative stress inhibits osteoblastic differentiation of bone cells by ERK and NF-kappaB. Biochem Biophys Res Commun 2004;314:197–207. [PubMed: 14715266]
57. Mody N, Parhami F, Sarafian TA, Demer LL. Oxidative stress modulates osteoblastic differentiation of vascular and bone cells. Free Radic Biol Med 2001;31:509–19. [PubMed: 11498284]
58. Krakauer JC, McKenna MJ, Buderer NF, Rao DS, Whitehouse FW, Parfitt AM. Bone loss and bone turnover in diabetes. Diabetes 1995;44:775–82. [PubMed: 7789645]
59. Suzuki K, Kurose T, Takizawa M, Maruyama M, Ushikawa K, Kikuyama M, Sugimoto C, Seino Y, Nagamatsu S, Ishida H. Osteoclastic function is accelerated in male patients with type 2 diabetes mellitus: the preventive role of osteoclastogenesis inhibitory factor/osteoprotegerin (OCIF/OPG) on the decrease of bone mineral density. Diabetes Res Clin Pract 2005;68:117–25. [PubMed: 15860239]
60. Orwoll ES. Osteoporosis in men. Endocrinol Metab Clin North Am 1998;27:349–67. [PubMed: 9669142]
61. Ahmed LA, Schirmer H, Berntsen GK, Fonnebo V, Joakimsen RM. Self-reported diseases and the risk of non-vertebral fractures: the Tromso study. Osteoporos Int 2006;17:46–53. [PubMed: 15838716]
62. el Miedany YM, el Gaafary S, el Baddini MA. Osteoporosis in older adults with non-insulin-dependent diabetes mellitus: is it sex related? Clin Exp Rheumatol 1999;17:561–7. [PubMed: 10544839]

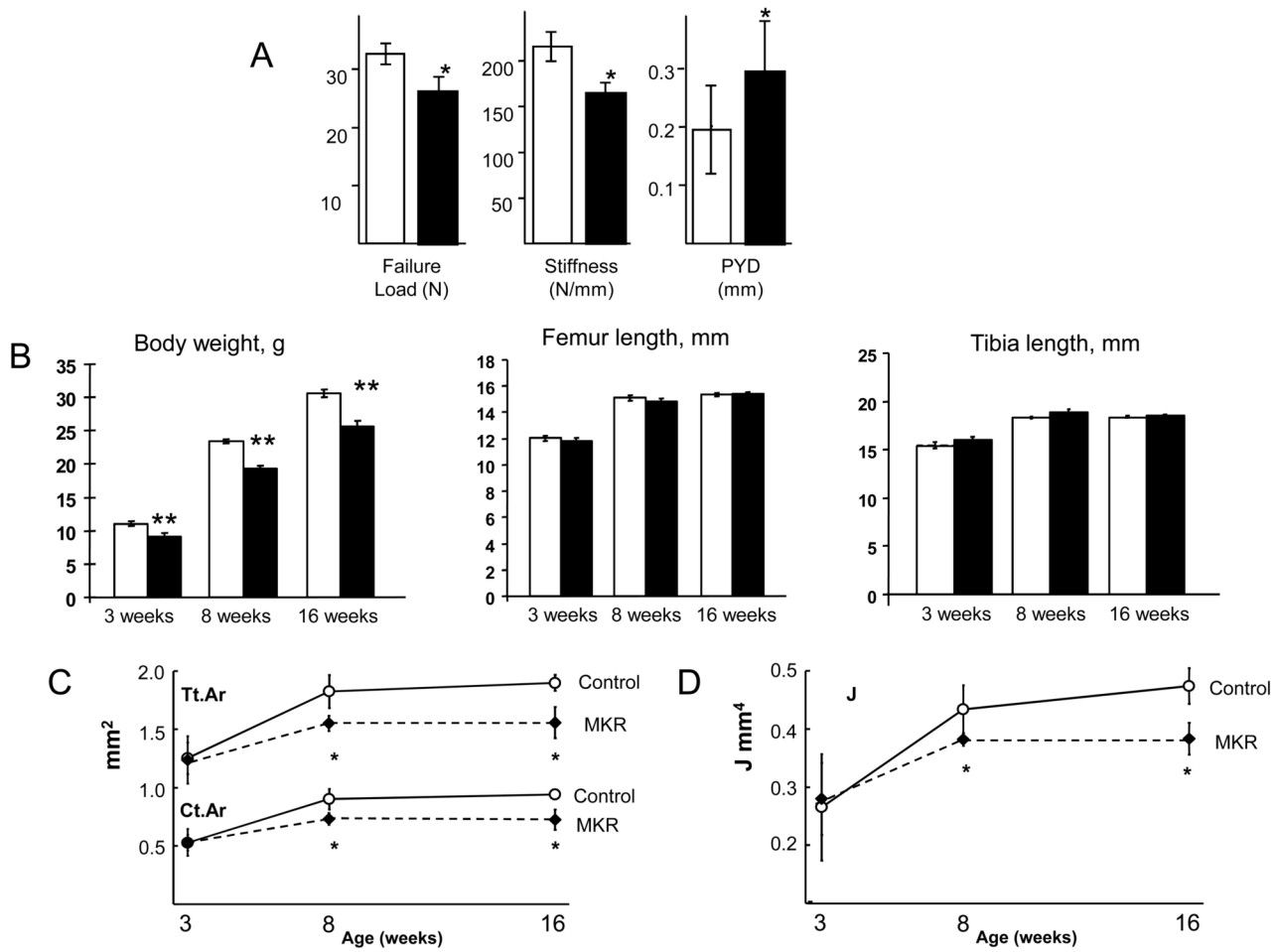

Figure 1.

(A) Adult MKR mice have femora that are weaker and less stiff than WT, but have greater post-yield deflection (PYD). Mechanical properties were quantified by loading 16 week-old mouse femora to failure in 4-point bending at 0.05 mm/sec using a servo-hydraulic materials test system (Instron Corporation), MKR (solid) and WT (open). Group means (+/− SD), n = 7–10 mice per group, *p<0.05. **(B)** (middle and right panels) The long bones of MKR mice have similar lengths as those of WT at 3, 8 and 16 weeks of age. Group means (+/− SD), n = 6–10 mice per group. **(C)** micro-CT of femora from WT and MKR mice revealed a slender shaft with similar length, but thinner cortices in MKR mice at 8 and 16 weeks of age (total area (Tt.Ar) and cortical area (Ct.Ar) for an equivalent long-bone length). **(D)** The lower stiffness and strength of femora from adult MKR male mice is due to greater structural slenderness, i.e., lower cross-sectional polar moment of inertia (J), when compared to wild-type (WT). Group means (+/− SD), n = 6–10 mice per group, *p<0.05.

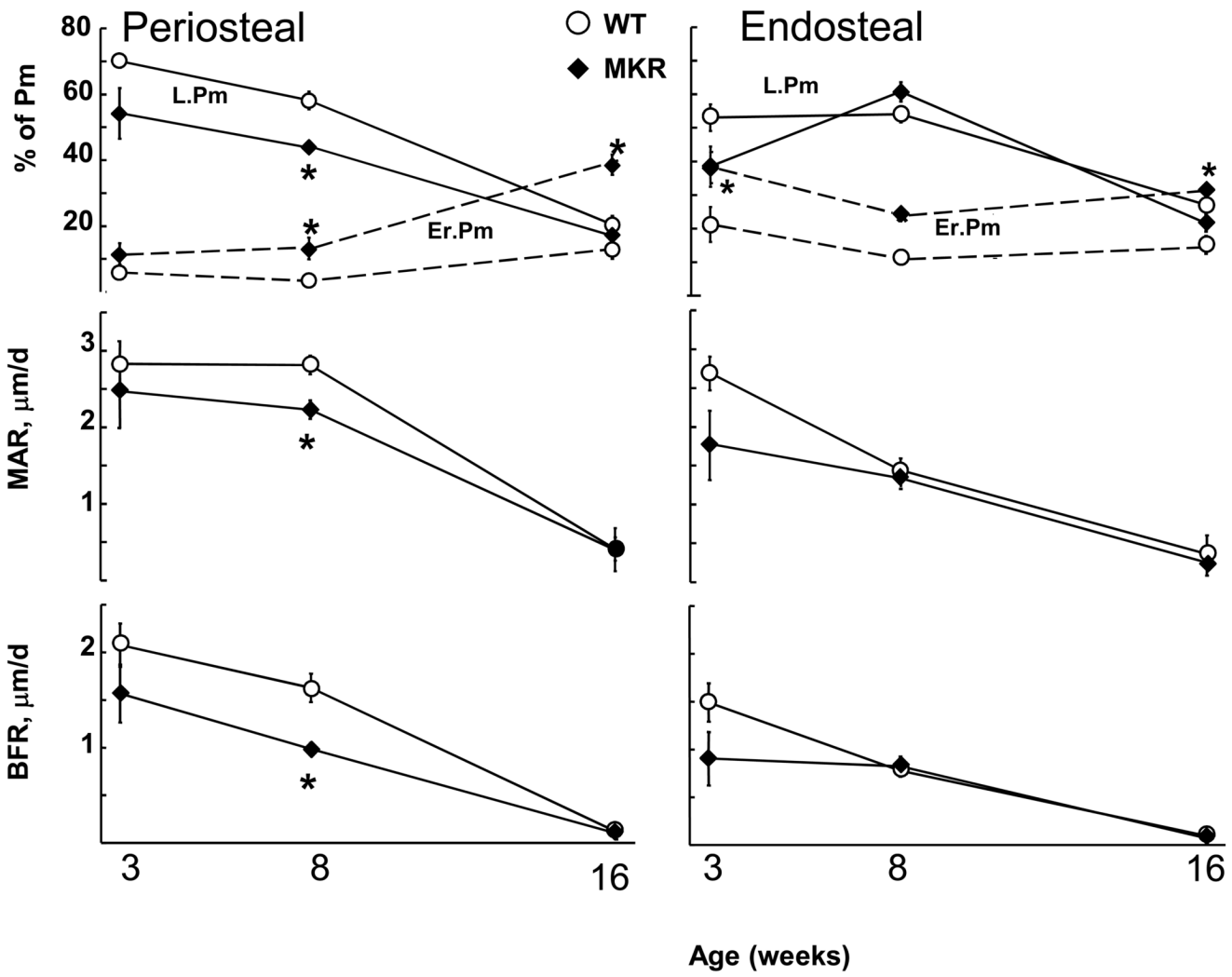

Figure 2.

The cellular mechanisms involved on cortical surfaces measured by periosteal and endosteal perimeters (Pm) of mid-shaft cross-sections. Lower osteoblast formation activity (% labeled perimeter, L.Pm), average osteoblast work (mineral apposition rate, MAR) and their product (bone formation rate, BFR=L.Pm*MAR) on the periosteal (left) surface during growth from 3 through 8 weeks of age as well as greater osteoclast resorption activity (% eroded perimeter, Er.Pm) on both periosteal and endosteal (right) surfaces contribute to slenderness and reduced stiffness of MKR versus WT. Group means (+/− SE), n = 6–8 mice per group,*p<0.05.

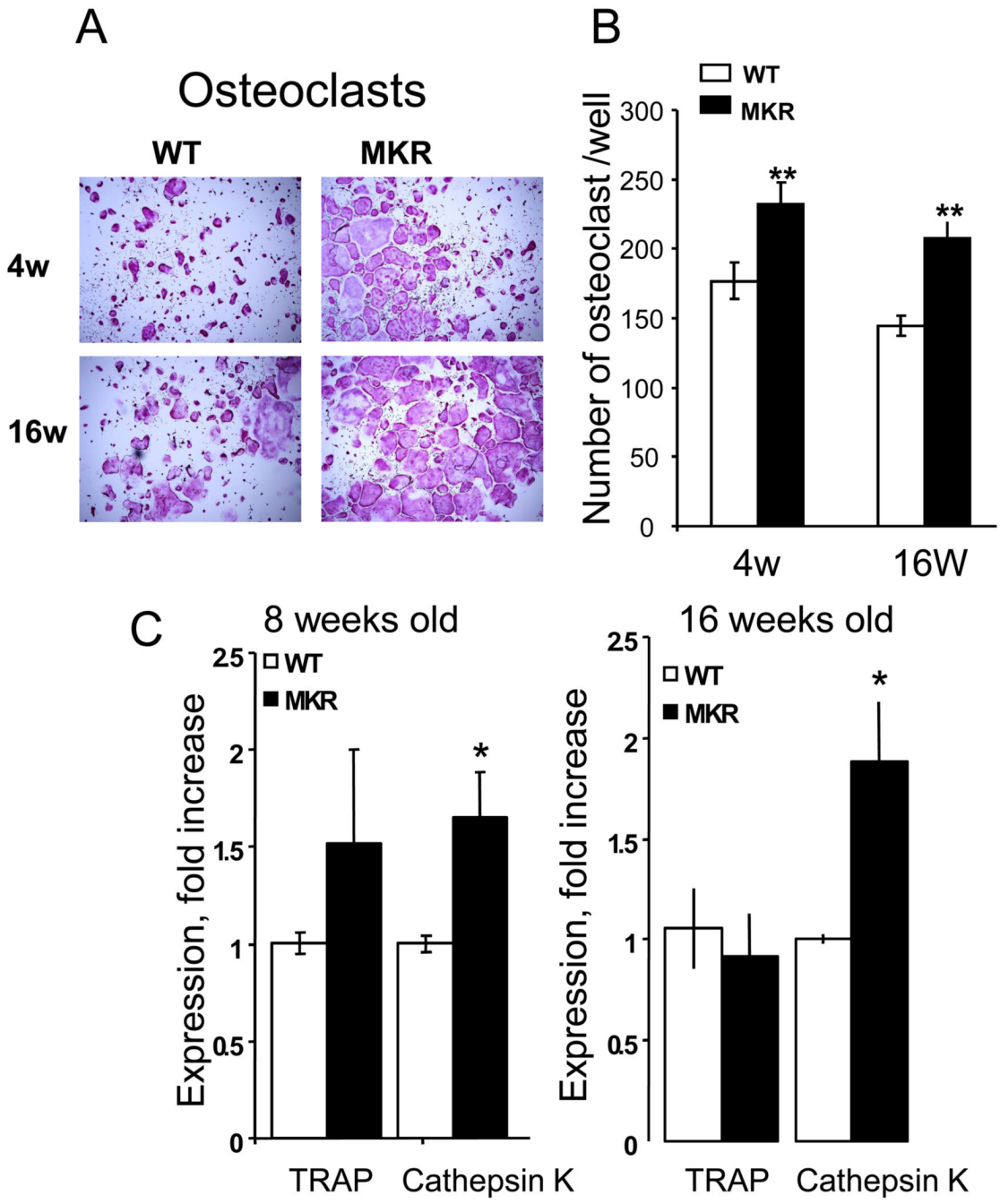

Figure 3.

(A) Representative images of 5 day osteoclast-like cultures derived from bone marrow of 4, and 16 week-old mice and (B) Multinucleated, TRAP positive osteoclasts were counted in cultures derived from bone marrow of 4, and 16 week-old mice (number of osteoclasts per well). (C) Expression levels of TRAP and cathepsin K were assessed by real-time PCR of 5 day osteoclast cultures derived from bone marrow of 8, and 16 week-old mice. Group means (+/− SE), n = 6–8 mice per group,*$p<0.05$).

Table 1

Mid-shaft cortical diaphyseal properties, femur length and body mass for WT and MKR mice

Variable	Age	WT	MKR	Δ (MKR-WT)	Δ/WT (%)
Tt.Ar (mm^2)	3 Week	1.25 (0.136)^b	1.24 (0.203)^b	−0.02	−2
	8 Week	1.86 (0.086)	**1.54** (0.065)^a	−0.32	**−17**
	16 Week	1.90 (0.068)	**1.56** (0.135)^a	−0.34	**−18**
Ma.Ar (mm^2)	3 Week	0.72 (0.077)^b	0.71 (0.107)^b	−0.02	−1
	8 Week	0.93 (0.060)	**0.82** (0.026)^a	−0.12	**−17**
	16 Week	0.96 (0.066)	**0.83** (0.054)^a	−0.12	**−18**
Ct.Ar (mm^2)	3 Week	0.53 (0.066)^b	0.53 (0.115)^b	0.00	−2
	8 Week	0.93 (0.037)	**0.72** (0.050)^a	−0.20	**−12**
	16 Week	0.94 (0.022)	**0.73** (0.088)^a	−0.22	**−13**
J (mm^4)	3 Week	0.27 (0.092)^b	0.28 (0.062)^b	0.01	0
	8 Week	0.44 (0.039)	**0.38** (0.010)^a	−0.06	**−22**
	16 Week	0.47 (0.031)	**0.38** (0.027)^a	−0.09	**−23**
Ct.Wi (mm)	3 Week	0.15 (0.012)^b	0.15 (0.023)^b	0.00	5
	8 Week	0.23 (0.007)	**0.19** (0.011)^a	−0.04	**−13**
	16 Week	0.23 (0.009)	**0.19** (0.018)^a	−0.04	**−19**
Es.Pm (mm)	3 Week	3.10 (0.174)^b	3.06 (0.243)^b	−0.04	1
	8 Week	3.66 (0.119)	**3.36** (0.089)^a	−0.30	**−16**
	16 Week	3.71 (0.136)	**3.33** (0.117)^a	−0.39	**−17**
Ps.Pm (mm)	3 Week	4.12 (0.306)^b	4.03 (0.311)^b	−0.08	−1
	8 Week	5.28 (0.334)^b	4.98 (0.362)	−0.30	−8
	16 Week	5.65 (0.507)	**4.82** (0.379)^a	−0.83	**−10**

Variable	Age	WT	MKR	Δ (MKR-WT)	Δ/WT (%)
TMDn (mg/cc)	3 Week	834 (26)[b]	869 (88)[b]	35	−2
	8 Week	993 (23)	960 (19)	−33	−6
	16 Week	1016 (33)	1005 (62)	−11	−1
Length (mm)	3 Week	11.91 (0.532)[b]	11.89 (0.364)[b]	−0.02	−4
	8 Week	15.16 (0.211)[b]	14.91 (0.146)[b]	−0.25	−3
	16 Week	15.50 (0.180)	15.46 (0.174)	−0.04	−1
Body mass (g)	3 Week	11.22 (0.539)[b]	**9.28** (0.648)[a,b]	−1.94	**−17**
	8 Week	23.53 (0.540)[b]	**19.42** (0.432)[a,b]	−4.11	**−17**
	16 Week	30.65 (0.754)	**25.68** (0.889)[a]	−4.97	**−16**

Data are presented as means (±SD). WT mice were FVB/N. Sample sizes were WT: 3 Week (n=6), 8 Week (n=9), 16 Week (n=7) and MKR: 3 Week (n=7), 8 Week (n=7), 16 Week (n=10). $p<0.05$:

[a] **versus age-matched WT** (significant MKR transgene effect);

[b] versus 16-week-old mouse of same phenotype (significant growth effect).

Table 2

Cancellous properties in the femur metaphyses of WT and MKR mice

Variable	Age	WT	MKR	Δ (MKR -WT)	Δ/WT (%)
Proximal Metaphysis					
BV/TV	3 Week	0.54 (0.09)[b]	**0.43 (0.11)**[a,b]	−0.12	**−21**
	8 Week	0.76 (0.08)	0.66 (0.14)	−0.10	−13
	16 Week	0.84 (0.04)	**0.63 (0.10)**[a]	−0.21	**−25**
Tb.Th (μm)	3 Week	33 (4)[b]	26 (4)[b]	−6.7	−21
	8 Week	59 (10)[b]	51 (14)	−8.1	−14
	16 Week	80 (9)	**51 (11)**[a]	−28.8	**−36**
Tb.Sp (μm)	3 Week	32 (8)[b]	40 (8)	7.4	23
	8 Week	26 (5)	36 (8)	7.0	27
	16 Week	24 (4)	**37 (9)**[a]	13.5	**58**
Distal Metaphysis					
BV/TV	3 Week	0.26 (0.03)	0.23 (0.03)[b]	−0.02	−9
	8 Week	0.20 (0.02)	0.17 (0.03)	−0.03	−17
	16 Week	0.23 (0.02)	**0.14 (0.02)**[a]	−0.09	**−40**
Tb.Th (μm)	3 Week	56 (5)	50 (2)	−6.0	−11
	8 Week	48 (2)	46 (2)	−1.8	−4
	16 Week	52 (3)	45 (2)	−7.4	−14
Tb.Sp (μm)	3 Week	165 (25)	167 (21)[b]	2.0	1
	8 Week	192 (14)	**247 (81)**[a]	54	**28**
	16 Week	172 (14)	**276 (26)**[a]	104	**60**

Data are presented as group means (±SD). WT mice were FVB/N. Sample sizes were WT: 3 Week (n=6), 8 Week (n=9), 16 Week (n=7) and MKR: 3 Week (n=7), 8 Week (n=7), 16 Week (n=10). $p<0.05$:

[a] **versus age-matched WT** (significant MKR transgene effect);

[b] versus adult, 16-week-old mouse of same phenotype (significant growth effect).